

Neutrino-Portal Dark Matter Detection Prospects at a Future Muon Collider

Jyotisma Adhikary,^{1,*} Kevin J. Kelly,^{2,†} Felix Kling,^{3,‡} and Sebastian Trojanowski^{1,§}

¹*National Centre for Nuclear Research, Pasteura 7, Warsaw, PL-02-093, Poland*

²*Department of Physics and Astronomy, Mitchell Institute for Fundamental Physics and Astronomy, Texas A&M University, College Station, TX 77843, USA*

³*Deutsches Elektronen-Synchrotron DESY, Notkestr. 85, 22607 Hamburg, Germany*

With no concrete evidence for non-gravitational interactions of dark matter to date, it is natural to wonder whether dark matter couples predominantly to the Standard Model (SM)’s neutrinos. Neutrino interactions (and the possible existence of additional neutrinophilic mediators) are substantially less understood than those of other SM particles, yet this picture will change dramatically in the coming decades with new neutrino sources. One potential new source arises with the construction of a high-energy muon collider (MuCol) – due to muons’ instability, a MuCol is a source of high-energy collimated neutrinos. Importantly, since the physics of muon decays (into neutrinos) is very well-understood, this leads to a neutrino flux with systematic uncertainties far smaller than fluxes from conventional high-energy (proton-sourced) neutrino beams. In this work, we study the capabilities of a potential neutrino detector, “MuCol ν ,” placed ~ 100 m downstream of the MuCol interaction point. The MuCol ν detector would be especially capable of searching for a neutrinophilic mediator ϕ through the mono-neutrino scattering process $\nu_\mu N \rightarrow \mu^+ \phi X$, exceeding searches from other terrestrial approaches for m_ϕ in the \sim few MeV – ten GeV range. Even with a 10 kg-yr exposure, MuCol ν is capable of searching for well-motivated classes of thermal freeze-out and freeze-in neutrino-portal dark matter.

I. INTRODUCTION

Neutrinos and their interactions reside among the largest open questions in fundamental physics today. The Standard Model (SM) of particle physics contains no definite mechanism by which neutrinos acquire mass which has driven immense experimental and theoretical activity since the observation of neutrino oscillations, a phenomenon that requires massive neutrinos. Simultaneous experimental and theoretical activity has scrutinized the completeness of the SM as a quantum field theory describing nature; if new physics exists between the scales of electroweak symmetry breaking and the Planck scale, it has yet to be discovered in our highest-energy facility, the Large Hadron Collider (LHC). One final mystery that remains unaddressed by the SM is the overwhelming evidence for dark matter (DM) in the universe; if it has interactions with the SM beyond gravitational ones, these are yet undetermined.

As experimental particle physics evolves, new strategies and approaches are continuously being developed to better understand fundamental particles and their interactions. One promising approach to address many of the aforementioned puzzles in the future is the construction of a muon collider (MuCol), capable of operation at several-TeV energies [1, 2]. While a great deal of physics can be explored by observing such high-energy muon-antimuon collisions, in this work, we focus on another

aspect of such facilities: the unavoidable source of collimated, high-energy neutrinos produced as a byproduct. Even with enormous Lorentz-boost factors, stored muons will decay quickly enough in these beamlines, leading to a well-characterized flux of neutrinos. By deploying a relatively small neutrino detector nearby, yet aligned with the muon beam, we have the opportunity to study the interactions of TeV-scale neutrinos with a well-understood flux, allowing for great sensitivity to new physics. Hereafter, we refer to this detector as MuCol ν .

One intriguing possibility that has garnered attention recently is that neutrinos, via some new mediator particle, carry the strongest interaction with dark matter particles. This situation has gained visibility for two major reasons: from a model-building perspective, it is not too difficult to postulate a neutrophilic mediator [3] in the \sim MeV-GeV mass range that couples strongly to neutrinos and dark matter, but not (at least not strongly) to charged SM fermions. Second, since neutrino interactions are the poorest-known among SM particles, there is ample possibility for novel interactions to exist. In this paper, we explore the possibility of detecting such a neutrinophilic mediator in the MuCol ν detector close by to a muon collider’s storage ring, using the potential for a connection to dark matter as additional motivation.

The main idea of this work is summarized in the left panel of Fig. 1. Muons in the straight parts of the beam pipe close to the interacting points will decay into a ν_μ and $\bar{\nu}_e$, forming an intense and strongly collimated beam in the forward direction. The ν_μ could scatter in a downstream detector located, placed ~ 100 m from the MuCol interaction point (IP), and produce the neutrinophilic scalar via the mono-neutrino process $\nu_\mu N \rightarrow \mu^+ \phi X$ which could be detected through the presence of a wrong-

* jyotisma.Adhikary@ncbj.gov.pl

† kjkelly@tamu.edu

‡ felix.kling@desy.de

§ sebastian.Trojanowski@ncbj.gov.pl

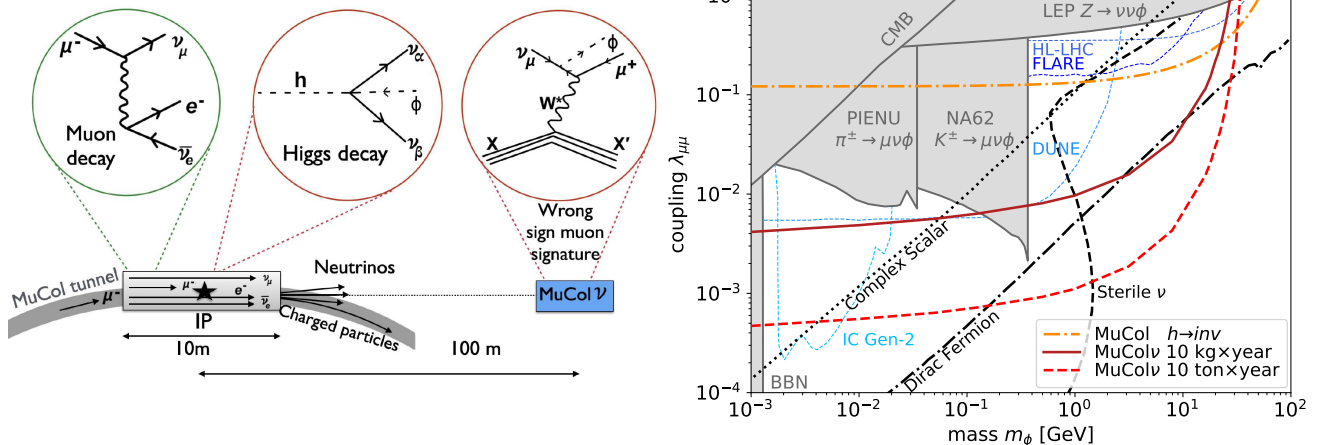


FIG. 1. **Left: Schematic diagram of the main focus of this paper.** In the left bubble, we show how stored muons in a muon collider (MuCol) tunnel decay into SM neutrinos. Downstream (right bubble), a hypothetical neutrino detector can search for mono-neutrino scattering with a wrong-sign muon due to emission of a lepton-number-charged mediator. Simultaneously (center), precision measurement of Higgs decays in the MuCol detectors can further constrain the new-physics scenario of interest. **Right: Landscape of the neutrinophilic mediator.** We show the sensitivity of neutrino scattering measurements using a 10 kg and 10 ton neutrino detector as well as precision measurements of the invisible decay width of the Higgs on the parameter space of the neutrinophilic mediator. Existing constraints are shown as gray shaded area while the projected sensitivity of other proposed searches is shown as blue dashed lines. See text for details.

sign muon in the final state. The sensitivity for both a 10 kg and 10 ton mass detector as estimated in this work are shown the right panel of Fig. 1. This clearly indicates the potential of a neutrino experiment at the muon collider to significantly exceed constraints obtained by past and planned searches and probe a variety of benchmarks scenarios in which the neutrinophilic mediator can explain the observed dark matter relic abundance. At the same time, precision measurements of the Higgs-to-invisible decay rates at the main detector of a muon collider would provide complementary sensitivity to the same new-physics scenario.

The paper is structured as follows. In Sec. II, we present the neutrinophilic mediator model and possible connections to dark matter as well as existing constraints and sensitivities of other proposed searches. In III we discuss how the neutrinophilic mediator can be probed by measuring neutrino interactions at a dedicated forward neutrino detector at a muon collider and obtain the resulting sensitivity. An alternative approach of testing neutrinophilic mediators using invisible Higgs decays at the MuCol is discussed in Sec. IV. We conclude in Sec. V.

II. NEUTRINOPHILIC MEDIATOR MODEL

In this work, we consider an additional neutrinophilic particle ϕ which couples neutrinos to one or more dark matter particles. Additionally, this mediator can lead to stronger-than-expected neutrino self-interactions. We begin with the assumption that ϕ carries lepton number -2 and its interactions with the SM arise from a

dimension-six operator [4],

$$\mathcal{L} \supset \frac{1}{\Lambda_{\alpha\beta}^2} (L_\alpha H) (L_\beta H) \phi + \text{h.c.}, \quad (1)$$

where $\Lambda_{\alpha\beta}$ is the scale at which this EFT breaks down, and we implicitly allow for some flavor dependence. After electroweak symmetry breaking, this generates several interaction terms in the Lagrangian – of particular interest here is the term

$$\mathcal{L} \supset \frac{1}{2} \lambda_{\alpha\beta} \nu_\alpha \nu_\beta \phi + \text{h.c.}, \quad (2)$$

where $\lambda_{\alpha\beta} = v^2/\Lambda_{\alpha\beta}^2$. Simultaneously, Eq. (1) generates an interaction term $\mathcal{L} \supset (\lambda_{\alpha\beta}/v) \nu_\alpha \nu_\beta \phi h$, which allows for Higgs boson decays into ϕ and a pair of neutrinos, assuming $m_\phi < m_h$. For the remainder of this work, we will assume for simplicity that $\lambda_{\mu\mu}$ is the only nonzero coupling – further discussion of alternative flavor-structure can be found in Ref. [3].

Assuming that ϕ also couples to dark matter, it may mediate dark matter/SM interactions and could set the dark matter relic abundance. We consider two scenarios.

Thermal freeze-out Dark Matter: Since ϕ carries lepton number -2 , dark matter particles interacting to ϕ must be charged as well. In some cases, this guarantees the stability of the dark matter [5]. Two such examples, explored thoroughly in Ref. [5], are that the dark matter is a Dirac fermion (DF) with lepton number $+1$ or a complex scalar (CS) with lepton number $+2/3$. In these two cases, the relevant interac-

tion terms in the Lagrangian are

$$\mathcal{L}_{\text{DF}} \supset \frac{1}{2}y\bar{\chi}^c\chi\phi + \text{h.c.}, \quad \mathcal{L}_{\text{CS}} \supset \frac{1}{6}y\chi^3\phi + \text{h.c.} \quad (3)$$

In both of these cases, with sufficiently strong neutrino-DM interactions, the dark matter will thermalize with the SM in the early universe. As the temperature of the plasma drops close to the DM mass, the DM-neutrino interactions will freeze out, and if the thermally-averaged cross section $\sigma v(\chi\chi \rightarrow \nu\nu)$ (DF) or $\sigma v(\chi\chi \rightarrow \chi^*\nu\nu)$ (CS) is of the correct size, the relic abundance today of χ could be responsible for the observed abundance of dark matter. For a given m_ϕ and m_χ this amounts to the product $y\lambda_{\alpha\beta}$ taking on a particular value. Ref. [5] found that, for $\sim\text{GeV}$ -scale masses for χ and ϕ , this amounts to $y\lambda_{\alpha\beta} \approx 10^{-2}$. Lines of constant $\Omega_\chi h^2$ satisfying the observed relic abundance of dark matter are shown for the DF (black, dot-dashed line) and CS (black, dotted line) cases in Fig. 1(right). Here we assume $y = 1$ and $m_\phi = 3m_\chi$ – see Refs. [5, 6] for more detail and for alternative choices regarding y and m_ϕ/m_χ .

Freeze-in Sterile-neutrino Dark Matter: An alternative possibility related to DM is that the mediator ϕ induces relatively large neutrino self-interactions that, coupled with mixing between the SM neutrinos and a new sterile neutrino ν_s , allows an abundance of ν_s to be populated over the thermal evolution of the universe. This is akin to the Dodelson-Widrow mechanism [7], augmented by these stronger self-interactions and has been explored, for instance, in Refs. [8–10]. In this regard, sterile neutrinos with ~ 10 keV masses and relatively small mixing with the SM can be adequately populated as DM with relatively large $\lambda_{\alpha\beta}$ that induce the self-interactions. However, this form of DM is in tension with the abundances of Milky-Way satellite counts [11]. Nevertheless, we view this freeze-in scenario as an interesting target for searches for the neutrinophilic mediator ϕ .

The interaction in Eq. (2) leads to neutrino-neutrino- ϕ vertices – however, since ϕ carries lepton number, the character of the neutrino interacting with ϕ “flips” from neutrino to antineutrino, or vice versa. In the following sections, we explore how this vertex allows for nontrivial neutrino-nucleus scattering [4, 5] that can be searched for in a variety of environments – specifically for this work, a muon-collider-sourced neutrino detector.

The neutrinophilic ϕ may be searched for in numerous ways when $\lambda_{\mu\mu} \neq 0$ – we summarize several of the leading constraints as a function of m_ϕ here, presented as shaded grey regions in Fig. 1 (right). For masses $m_\phi \lesssim \text{MeV}$, ϕ can be thermalized with the SM and remain in contact throughout big-bang nucleosynthesis. If so, ϕ will act as (approximately) an additional degree of relativistic radiation throughout light-element formation, which is severely constrained for $m_\phi < 2$ MeV [12]. On the other hand, neutrino self interactions can also leave imprints

on the Cosmic Microwave Background (CMB). The gray shaded region in the parameter space is excluded by the current CMB data [13]. The parameter space is also constrained by rare decays of $Z \rightarrow \nu_\mu\nu_\mu\phi$ [14] and mesons $M^\pm \rightarrow \mu\nu_\mu\phi$ [4, 15] by the PIENU [16] and NA62 [17] for rare π^\pm and K^\pm decays, respectively.

Detecting high-energy astrophysical neutrinos with IceCube has provided a unique avenue to explore neutrino self-interactions, despite current constraints being weaker than laboratory probes. Future observatories like IC-Gen2 promise significant improvements in sensitivity [18]. The DUNE facility which will have an intense beam of neutrinos (but largely uncontaminated by antineutrinos) with energies of a few GeV and will be able to study neutrino BSM signature as discussed in this paper looking for wrong sign muon with the help of liquid argon near detector [4, 5]. On the other hand, in the far forward region of LHC, at the FLArE detector at the Forward Physics Facility (FPF), the same BSM signature will be probed [6, 19]. However, due to the presence of both neutrinos and antineutrinos in the beam, FLArE will mainly look for missing energy signatures. Another interesting channel to look for the scalar mediator is $h \rightarrow \nu\nu\phi$ and $h \rightarrow \bar{\nu}\bar{\nu}\phi$ decays. Both LHC at High Luminosity era [20] and MuCol as discussed in the upcoming section will be able to probe this decay channel. In our analysis, we focus on a MuCol colliding opposite-sign muons – a same-sign muon collider [21] has very strong sensitivity in the same parameter space we explore by searching for signals of apparent lepton-number violation and missing energy, as emphasized in Ref. [22].

III. NEUTRINO SCATTERING SIGNALS

In this section, we focus on the neutrino-induced signature related to the BSM scalar introduced in Eq. (2). We first briefly discuss the neutrino detector concept used in our analysis. We then present the new physics signal and backgrounds and provide a detailed analysis of how to discriminate between them.

Neutrino Detection at the Muon Collider

Any circular muon collider naturally consists of a muon storage ring that would deliver the beam to the collision points. Due to their short lifetime, the stored muons will decay and produce a large number of neutrinos. This makes a muon collider a powerful neutrino source.

In this study, we will use the neutrino fluxes obtained for a muon collider with a center-of-mass energy of 3 TeV as presented in Ref. [1]. This design envisions a 4.5 km long storage ring into which about 10^{13} muons will be injected each second. While these muons can decay anywhere in the ring, the largest flux of neutrinos originates from decays in the straight sections around the IPs. We

conservatively assume that the straight section have a length of 10 m, resulting in about 10^{10} neutrinos per second. This exceeds the flux predictions for ongoing and future forward neutrino detectors at hadronic colliders by several orders of magnitude [23–26]

The neutrinos produced in muon decay will have a transverse momentum similar to the muon mass and typical energies of 100 GeV or more. The neutrino beam is then highly collimated with an angular spread of $m_\mu/E_\nu \lesssim 1$ mrad. Therefore, even a relatively small cylindrical detector with radius $R = 10$ cm placed 100 m downstream from IP and centered on the muon beam collision axis is sufficient to encompass the entire beam. Detectors placed further away with correspondingly larger transverse size would lead to the same sensitivity.

Crucially, the MuCol ν detector placed on one side of the IP at the collider will capture essentially pure samples of muon neutrinos ν_μ and electron antineutrinos $\bar{\nu}_e$, while the corresponding antiparticles, $\bar{\nu}_\mu$ and ν_e , will be produced in the opposite direction from the IP. This directional separation plays an important role in mitigating backgrounds, as discussed below; see also Ref. [27] for a similar discussion in the context of a muon fixed-target experiment at the MuCol. Notably, forward neutrinos at the MuCol have a narrower energy spread than those at hadronic colliders, and their spectrum can be predicted with greater accuracy (given that they come from the well-known three-body muon decay), reducing the corresponding systematic uncertainties in neutrino measurements. We assume that these uncertainties can be further suppressed by measuring the dominant charge current (CC) neutrino interaction rates, rendering them negligible in our analysis.

A preliminary neutrino detector concept for muon storage rings and colliders, proposed in Ref. [28], consists of a 1 m long cylindrical detector with a 10 cm radius. It comprises 750 silicon CCD tracking planes followed by a magnetized spectrometer and calorimeter. This design aims to ensure strong tracking and reconstruction capabilities, as well as c/b -quark tagging. In this concept, the silicon target mass used for neutrino vertex detection is only 10 kg. However, interleaving the active target with denser materials could significantly increase this mass and, consequently, the expected neutrino interaction rate.

We present our results for two representative MuCol ν detector masses: 10 kg and 10 ton. For each, we study the expected BSM signal and backgrounds per year of MuCol operation. The larger detector mass is equivalent to, for example, a 1 ton detector operating for 10 years, accumulating the same total number of interactions. This 1 ton target mass is similar to that of the currently operating forward neutrino detectors at the LHC [29–31]. For simplicity, we assume iron target nuclei in our analysis. However, the results are largely driven by the detector mass and only mildly dependent on the specific nucleus.

Signal and Background

Our key signature is the process $\nu_\mu N \rightarrow \mu^+ \phi X$ in the MuCol ν detector, as illustrated in Fig. 1. This process, and many of the key observables with which it can be separated from neutrino-scattering backgrounds, has been explored in detail in Refs. [4–6]. In this section, we emphasize the ways in which the MuCol neutrino source and the MuCol ν detector excel in a search of this type. For instance – the scalar carries lepton number and escapes detection, so the interaction mimics a lepton-number-violating process. Because of the pure ν_μ beam produced by the MuCol (without contamination from $\bar{\nu}_\mu$), as well as the magnetization of the MuCol ν spectrometer, we expect exquisite capabilities using this approach.

We calculate the relevant cross sections using MadGraph5_aMC@NLO v2.9 [32] and employ the nCTEQ15 nuclear parton distribution function (PDF) set for the iron target nucleus [33]. Pythia8 [34] is used to further model the parton shower and hadronization for the signal events. We have validated the numerical results against a semi-analytical estimates based on the partonic cross sections provided in Refs. [6]. For small scalar masses and transverse momenta $m_\phi \ll p_{T_\phi} \sqrt{s}$, the scalar production cross section in neutrino-nucleon scattering approximately scales as

$$\sigma(\nu_\mu n \rightarrow \mu^+ \phi X) \simeq 10^{-37} \text{ cm}^2 \times \lambda^2 \times \frac{E_\nu}{\text{TeV}}, \quad (4)$$

where λ is the scalar coupling to neutrinos and E_ν is the incident neutrino energy.

Pythia8 is also employed to model neutrino-induced backgrounds. These backgrounds include charged current and neutral current (NC) scatterings of ν_μ and $\bar{\nu}_e$ that can occasionally lead to positive muons in the final state, among other visible products. This is dominantly due to neutrino-induced charm meson production with subsequent decays into muons. Approximately 10% of all CC ν_μ interactions at multi-100 GeV energies have a charm quark in the final state, $\nu_\mu s \rightarrow \mu^- c$, and about 10% of charm hadrons decay semileptonically to muons, $D^+, D^0 \rightarrow \mu^+ + X$ [35]. Hence, roughly 1% of all CC ν_μ events are expected to produce a positively charged muon. In contrast, the suppression is larger for NC events and CC $\bar{\nu}_e$ scatterings, as the lower c quark PDF suppresses the production rate of charm quarks in these processes. An additional source of positively charged muons are rare light meson decays, such as $\eta \rightarrow \mu^+ \mu^- \gamma$ or $\omega \rightarrow \mu^+ \mu^-$. However, these particle do not necessarily carry a large momentum fraction and the muons therefore tend to be less energetic. Crucially, all these backgrounds initially dominate over the expected BSM signal by several orders of magnitude. Below, we discuss in detail a possible background mitigation strategy that allows for isolating new physics events.

In addition to backgrounds with positive muons, neutrino interactions can mimic signal events through other processes. For instance, charged pion π^+ mis-

reconstruction could lead to a false muon signal. We assume that the detector’s muon identification and charged pion discrimination capabilities are sufficient to suppress such backgrounds. Furthermore, charged pions can decay into muons within the detector before being identified. To reject these backgrounds, sufficient angular resolution is necessary to identify in-flight pion decays by observing the momentum kink between the incident pion and outgoing muon tracks. A detailed analysis of these displaced backgrounds, which are highly dependent on the detector design, is left for future work. In the following, we focus on the *prompt* ν -induced backgrounds, in which μ^+ is produced close to the neutrino scattering vertex.

Neutrino event rates presented below are subject to uncertainties in modeling ν interactions, particularly the relevant cross section. These uncertainties, however, typically do not exceed a few percent for TeV-scale energies [36]. They are also expected to be further reduced by the time the MuCol ν detector operates, thanks to the data gathered in the neutrino physics program at the LHC [37] as well as measurements at the planned electron-ion collider (EIC) [38]. Therefore, we assume these uncertainties will not significantly affect the considered BSM search and neglect their impact in the following analysis. Finally, we include the effects of finite energy measurement resolution by smearing the momenta of outgoing particles produced in neutrino interactions. We assume Gaussian smearing with a 10% relative uncertainty on the measured energy for all particles.

Analysis

As discussed earlier, neutrino-induced backgrounds dominate over the BSM signal and must be rejected in the analysis. To illustrate how background can be suppressed, we first perform a simple-cut-and-count analysis using several key observables. To further improve the rejection and optimize the analysis performance, we also perform a multivariate analysis using a Boosted Decision Tree (BDT). The number of background events remaining after successive cuts is summarized in Table I. These results correspond a 10 kg MuCol ν detector operating for a year and are provided separately for CC and NC interactions of incident ν_μ and $\bar{\nu}_e$. The table also shows the signal efficiency (fraction of surviving events) for two representative masses of the BSM scalar, $m_\phi = 1$ or 20 GeV.

As a first step, we identify candidate signal events by requiring the presence of a positively charged muon and the absence of a negatively charged muon:

Positive muon: We require at least one positive muon in the final state of the neutrino interaction. To ensure its proper identification and a reliable energy measurement, we require a sufficiently high muon energy, specifically $E_{\mu^+} > 30$ GeV. This allows the positive muon to escape the target material and traverse the magnetized spectrometer and the muon system, i.e., a dedicated detector component designed to identify

muons and precisely measure their momenta. The magnet can deflect low-energy charged particles before they reach the muon system. This energy threshold is chosen based on a similar analysis for the FASER spectrometer at the LHC, which resembles the assumed MuCol ν detector setup [39].

Notably, imposing a minimum energy threshold on μ^+ has a minor impact on the BSM signal events, resulting in no more than a few percent suppression. However, this threshold significantly reduces the background event rate. As discussed earlier, about 1% of CC ν_μ interactions produce a μ^+ in the final state. Indeed, by requiring the presence of the positive muon, we observe a suppression of the corresponding background event rate by approximately two orders of magnitude. In this case, the positive muons often come from decays of leading charm hadrons, i.e., those with the largest momentum. Consequently, the energy threshold has a less pronounced impact on suppressing these events. For the other background types, the fraction of scattering events containing a charm quark are significantly lower and positive muon, originating from sub-leading charm hadrons or decays of lighter mesons produced in hadronic showers, are typically softer. In these cases, the requirement to have a muon with $E_{\mu^+} > 30$ GeV suppresses background event rates by three or even four orders of magnitude.

Negative muon: The leading background at this stage originates from CC ν_μ interactions. Unlike the signal, these are expected to contain an energetic negatively charged muon. We therefore veto events containing negative muons with energies above 30 GeV. This threshold is, again, chosen based on the assumed detector’s ability to reliably identify muons. While soft negative muons ($E_{\mu^-} < 30$ GeV) may be present in both signal and background events, their identification is less reliable, and thus no further cuts are applied on them.

While this requirement reduces the CC ν_μ background by more than an order of magnitude, it has a negligible impact ($< 1\%$) on the signal event rate. This minimal impact holds true for both $m_\phi = 1$ GeV and $m_\phi = 20$ GeV, as the ϕ scalar, especially at higher masses, is expected to carry a significant portion of the incident neutrino energy, leaving less energy available for the visible final-state particles.

These baseline identification conditions significantly reduce the background event rate (by over three orders of magnitude) while maintaining a high signal detection efficiency (greater than 90%), as shown in Table I. To further suppress backgrounds, we introduce additional cuts on the identified candidate signal events:

$E_{\mu^+}/E_{\text{vis}} > 0.5$: In the BSM signal events, the positive muon originates from the leptonic vertex in neutrino-nucleus scattering, distinct from μ^+ production in the hadron decays characteristic for background events.

Cut	Background Rates [Evt./((10 kg yr))]					Signal Efficiency for m_ϕ	
	CC ν_μ	CC ν_e	NC ν_μ	NC ν_e	All	1 GeV	20 GeV
All Events	$1.33 \cdot 10^7$	$5.57 \cdot 10^6$	$4.21 \cdot 10^6$	$2.03 \cdot 10^6$	$2.52 \cdot 10^7$	1.00	1.00
$E_{\mu^+} > 30$ GeV	$8.82 \cdot 10^4$	$2.24 \cdot 10^2$	$5.35 \cdot 10^3$	$2.39 \cdot 10^3$	$9.62 \cdot 10^4$	0.96	0.933
$E_{\mu^-} < 30$ GeV	$5.37 \cdot 10^3$	$1.11 \cdot 10^2$	$5.01 \cdot 10^3$	$2.23 \cdot 10^3$	$1.27 \cdot 10^4$	0.957	0.933
$E_{\mu^+} > 0.5 E_{\text{visible}}$	$2.73 \cdot 10^2$	0.298	$1.52 \cdot 10^2$	89.67	$5.15 \cdot 10^2$	0.628	0.464
charm veto	54.92	0.252	33.17	19.68	$1.08 \cdot 10^2$	0.606	0.463
p_{T,μ^+} vs. $\Delta\phi$	4.51	0.141	3.69	3.5	11.83	0.48	0.314
BDT	1.09	0.02	1.03	0.883	3.02	0.482	0.249

TABLE I. Event yields for background processes and the signal efficiency after consecutive cuts obtained for a 10 kg MuCol ν detector placed in the forward kinematic region of the MuCol and one year of data collection. Results are shown for charged current (CC) and neutral current (NC) neutrino scatterings of ν_μ and $\bar{\nu}_e$, and for two masses of the neutrinophilic scalar, $m_\phi = 1$ and 20 GeV.

Consequently, one expects that in signal events, μ^+ typically carries a more significant fraction of the total visible energy, E_{vis} .

This is illustrated in the top left panel of Fig. 2, which shows the distribution of interacting neutrinos in bins of the ratio E_{μ^+}/E_{vis} . Background events from CC and NC neutrino scatterings are shown in blue and red, respectively. These events have satisfied the baseline conditions on the presence and absence of positive and negative muons. For comparison, the corresponding distribution for the BSM scalar with $m_\phi = 1$ GeV and $\lambda = 0.3$ is also shown.

The ratio E_{μ^+}/E_{vis} provides strong discrimination between signal and background events. In particular, requiring $E_{\mu^+}/E_{\text{vis}} > 0.5$ reduces the NC ν_μ and both the CC and the NC $\bar{\nu}_e$ background event rates by approximately two orders of magnitude. The suppression is less effective for CC ν_μ scattering events, where μ^+ can be produced in decays of the leading charm hadron. However, the reduction still exceeds one order of magnitude in this case. We expect $\mathcal{O}(500)$ background events to survive this cut and mimic the signal.

The impact of the cut on signal efficiency depends on the BSM scalar mass, ranging from approximately 60% to 45% for the benchmark masses of 1 and 20 GeV, respectively. Notably, similar background rejection and signal detection efficiencies would not be achieved by using the positive muon energy E_{μ^+} or the visible energy E_{vis} alone. Both quantities decrease with increasing BSM scalar mass, as ϕ carries away a progressively larger fraction of the incident neutrino energy. Consequently, the efficiency of such cuts depends more strongly on m_ϕ . This dependence is partially mitigated by using the ratio of the two quantities in the analysis.

Charm tagging: As discussed above, energetic positive muons in background events are typically associated with a parent hadron carrying even higher energy. Sufficiently long-lived hadrons, such as charm mesons, can be identified in the detector based on their displaced decay. Therefore, charm tagging provides additional

discrimination against these backgrounds.

The proposed MuCol ν detector incorporates multiple high-resolution tracking planes capable of identifying these displaced vertices. In our analysis, we apply a charm tagging requirement with an assumed efficiency of 80% for hadrons decaying to μ^+ . Events induced by B -meson and τ -lepton decays are similarly rejected. The mistagging rate is assumed to be negligible for the BSM signal rate estimation. This selection reduces backgrounds by approximately a factor of five. However, as we will demonstrate later, charm tagging does not play a critical role in our multivariate analysis, which is significantly enhanced by the use of the BDT.

Transverse observables: Massive BSM neutrinophilic scalars can naturally be produced with substantial transverse momentum, $p_T \sim m_\phi$, which can be measured even in interactions of high-energy neutrinos. The presence of this missing transverse momentum alters the kinematics of ν scattering and can be used to discriminate against backgrounds.

In particular, the top right panel of Fig. 2 shows the distribution of the angle $\Delta\phi$ between the transverse momentum of the final-state positive muon, p_{T,μ^+} , and the missing transverse momentum, $p_{T,\text{miss}}$. In the background NC events, $p_{T,\text{miss}}$ is dominated by the outgoing neutrino, which recoils against the hadronic system containing the final-state μ^+ . Consequently, this angle exhibits a strong peak near $\Delta\phi \sim \pi$ (red histograms in the plot), indicating a preference for back-to-back topology in the transverse plane. In contrast, BSM signal events have a much broader $\Delta\phi$ distribution, given the presence of both energy associated with the undetected ϕ and μ^+ emerging from the leptonic vertex in the neutrino interaction. Signal events can then be effectively discriminated from the NC backgrounds by rejecting events with back-to-back topology.

Fig. 2 also shows the individual p_{T,μ^+} and $p_{T,\text{miss}}$ distributions in the bottom panels. These distributions illustrate that both variables could be used to further disentangle the BSM signal and CC background events

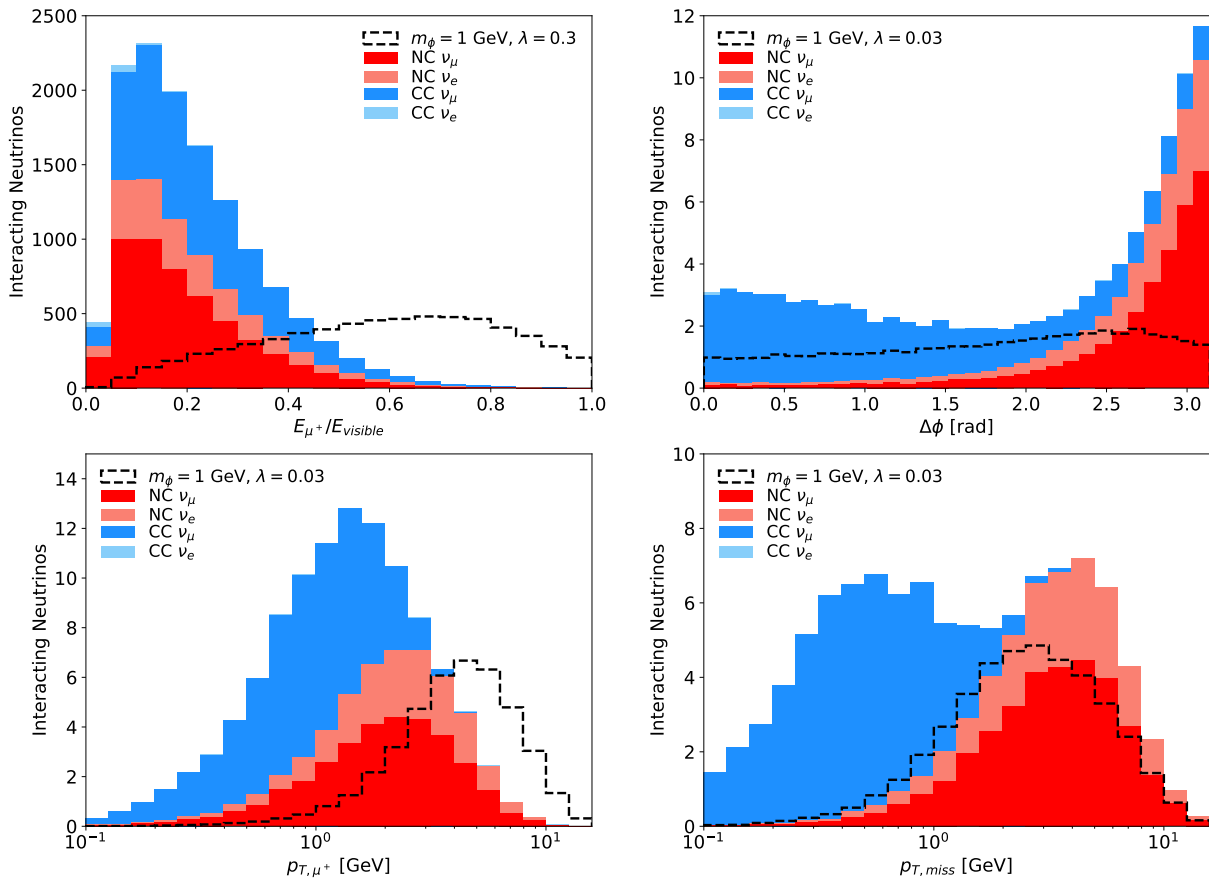


FIG. 2. Distributions of selected kinematic variables used in the analysis of neutrino-nucleus interactions within a proposed 10 kg MuCol ν detector at a 3 TeV muon collider. Stacked histograms show the predicted number of events per year. The distributions are shown for: the ratio between the positive muon and total visible energies, E_{μ^+}/E_{vis} (**top left**); the angle between the μ^+ and missing transverse momenta, $\Delta\phi$ (**top right**); the transverse momentum of the positive muon, p_{T,μ^+} (**bottom left**); and the missing transverse momentum, $p_{T,\text{miss}}$ (**bottom right**). Charged-current (CC) and neutral-current (NC) neutrino-induced background events are shown in blue and red, respectively and stacked in histograms. Dark and light shading within the histograms differentiates between muon neutrinos ν_{μ} and electron antineutrinos $\bar{\nu}_e$. Sample distributions for BSM signal events, indicated by black dashed lines, assume a scalar mass $m_{\phi} = 1$ GeV and a coupling strength $\lambda = 0.3$ (top left) or 0.03 (other panels).

(blue histograms). The distribution of the muon transverse momentum appears to be a more effective discriminant in this analysis. In addition, it also exhibits a weaker dependence on m_{ϕ} .

We examine the correlations between $\Delta\phi$ and p_{T,μ^+} , shown in Fig. 3 to improve signal detection and background rejection efficiency further. Since background ν -induced events typically have lower p_{T,μ^+} than the BSM signal, and NC events with high p_{T,μ^+} prefer $\Delta\phi \sim \pi$, we isolate signal events by focusing on the following kinematic region: $p_{T,\mu^+} > 2$ GeV and $p_{T,\mu^+} > 250 \text{ MeV} \times e^{\Delta\phi}$. This reduces the background event rate by an additional order of magnitude to the level of $\mathcal{O}(10)$ events in the 10 kg detector per year.

The overall background suppression of the presented analysis corresponds to six orders of magnitude, while the signal detection efficiency can be kept high, of about

30 – 50%, depending on the ϕ mass. While this analysis demonstrates how signal and SM background can be separated using simple physics-motivated cuts, an optimized multivariate analysis that considers additional correlations between the observables can further improve signal acceptance and background rejection.

BDT: To this end, we employ the BDT implemented in the SCIKIT-LEARN package [40]. Candidate signal events are preselected to have at least one μ^+ but no μ^- with energy $E > 30$ GeV, as discussed above. For each event, the following observables are considered: i) the muon energy E_{μ^+} ; ii) the visible energy E_{vis} ; iii) the energy deposited in electromagnetic showers E_{EM} ; iv) the positive muon transverse momentum p_{T,μ^+} ; v) the missing transverse momentum $p_{T,\text{mis}}$; vi) the scalar sum of all visible final state particle transverse momenta H_T ; vii) the angle between the positive muon and missing transverse momenta $\Delta\phi$; and viii) the con-

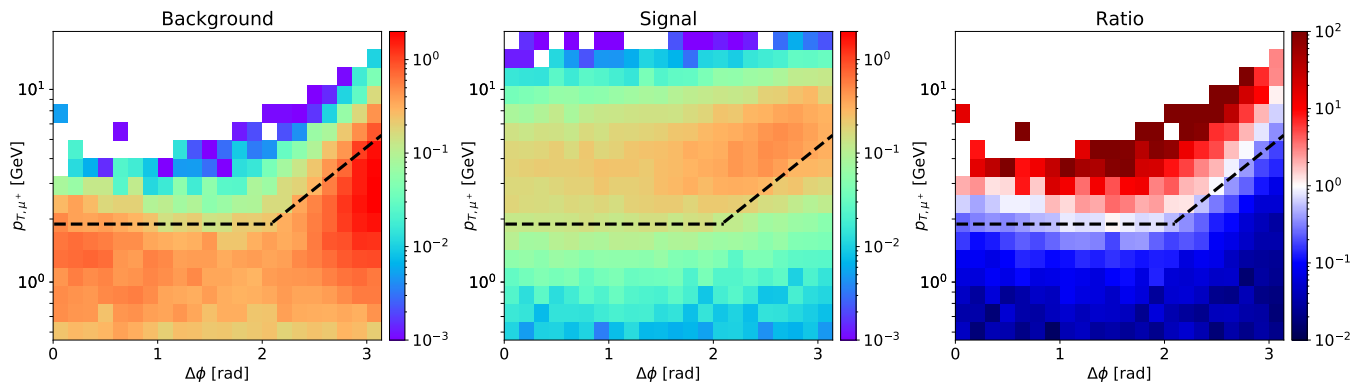


FIG. 3. Two-dimensional distributions of transverse observables used in the analysis, depicting the correlation between the angle between the μ^+ and missing transverse momenta, $\Delta\phi$, and the positive muon transverse momentum, p_{T,μ^+} . The figure compares background events (**left**) to BSM signal events (**center**) obtained assuming $m_\phi = 1$ GeV and $\lambda = 0.03$. The ratio of signal to background events is also presented (**right**).

dition whether or not the event was charm tagged (assuming a 80% charm tagging efficiency). The BDT was configured with 200 estimators, a maximal depth of 3, and a learning rate of 0.03. These hyperparameters were determined through a coarse scan, but no further optimization was performed. The event set was split equally into training and testing samples, with similar performance observed for both.

As shown in the left panel of Fig. 4, the BDT output variable provides good separation between signal and background. Applying a cut at > 0.7 on this variable reduces the background event rate to only a few events, cf. Table I, while maintaining a signal efficiency between 50% (low mass of ϕ) and 25% (high mass). In the case of the 10 ton detector, due to larger event rates, a stronger cut of > 0.9 was chosen in order to guarantee better discrimination power.

Interestingly, a feature importance analysis reveals that the separation is strongly driven by the transverse observables p_{T,μ^+} and $\Delta\phi$ as well as the muon energy E_{μ^+} . On the other hand, charm tagging plays a minor role. We have checked that very similar results can be obtained by not using charm tagging at all. This is an important consideration for potentially planning a larger 10-ton detector, which may have limited charm tagging capabilities. As the BDT study demonstrates, this limitation should not hinder the discovery potential of such a detector in the search for neutrinophilic scalars.

Sensitivity & Discussion

The right panel of Fig. 4 illustrates the projected exclusion bounds on the neutrinophilic scalar, obtained with a 10 kg MuCol ν detector and one year of MuCol operation at a center-of-mass energy of 3 TeV. To derive these

bounds, we require a signal-to-background ratio satisfying $S/\sqrt{B} > 2$ and a minimum of three signal events, $S > 3$.

The plot demonstrates the impact of consecutive cuts introduced in the analysis. Although the number of neutrino-induced background events is initially large, it can be significantly suppressed by imposing simple signal selection conditions on the muons (μ^+ and μ^-), as previously discussed. This alone allows us to probe new regions in the parameter space of the neutrinophilic scalar model, as shown by the red dotted line. Adding a further cut on the visible energy fraction carried by the positive muon, $E_{\mu^+}/E_{\text{vis}} > 0.5$, yields the improved bound indicated by the red short-dashed line. Rejecting charm-tagged events further enhances the sensitivity, leading to the bound depicted by the red dash-dotted line. Finally, incorporating constraints on transverse observables, cf. Fig. 3, produces the strongest bound from our cut-and-count analysis, represented by the red long-dashed line.

Employing the BDT yields even stronger bounds, as shown by the orange solid line. These constraints are only about a factor of two less stringent in λ compared to the ultimate sensitivity of the 10 kg detector, illustrated by the black dotted line, which assumes perfect background rejection and signal detection efficiency.

Fig. 1 also displays these BDT bounds as representative projections for two considered masses of the MuCol ν detector. Increasing the detector mass from 10 kg to 10 ton improves the projected bound by approximately an order of magnitude. While the number of expected BSM signal events scales as $N_{\text{sig}} \propto \lambda^2$ and increases roughly proportionally to the detector mass, the improvement in the bound is less than the naively expected factor of $10^{3/2} \approx 30$. This is due to the increased difficulty of suppressing ν -induced backgrounds in the larger detector, where the expected background rate after the BDT cut is $\mathcal{O}(100)$ events, compared to $\mathcal{O}(1)$ events in the smaller detector.

Nevertheless, these detectors can probe regions of the

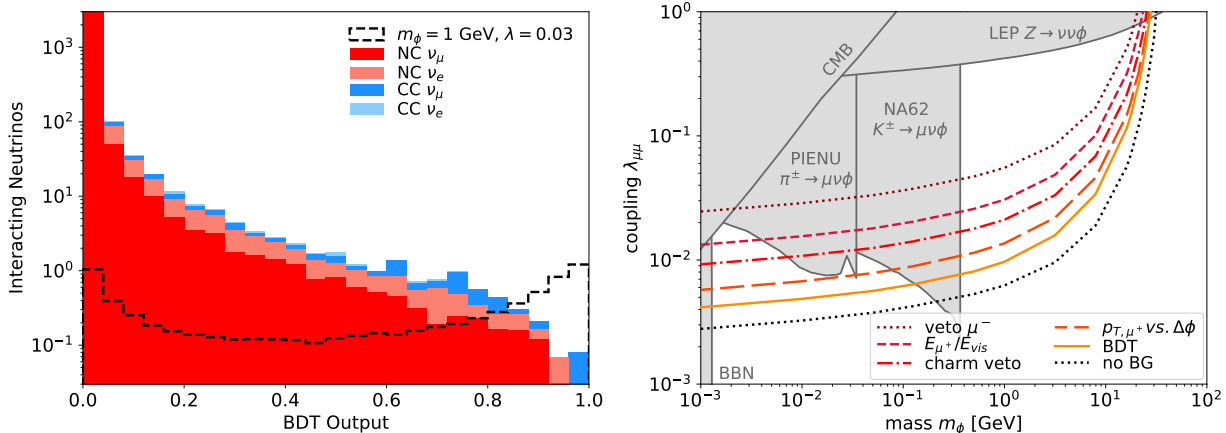


FIG. 4. **Left: BDT output variable distribution.** Similar to Fig. 2, but the distributions of the BDT score are shown for background and signal events. The latter correspond to the neutrinophilic scalar with $m_\phi = 1$ GeV and $\lambda = 0.03$. **Right: Projected exclusion bounds for various cuts.** Projected exclusion bounds obtained for the 10 kg MuCol ν detector at the Muon Collider operating for one year. From top to bottom, the lines represent the impact of adding consecutive cuts on kinematic variables discussed in the text, as indicated in the plot. The best-expected constraints are obtained with the BDT analysis and shown with the orange solid line. The black dotted line represents an ultimate limit obtained, assuming that backgrounds can be suppressed to negligible levels without affecting the number of signal events.

parameter space of the model inaccessible to other proposed searches. For comparison, we show projected bounds for DUNE [4, 5], IC Gen-2 [18], and FLArE [6]. Notably, even the small 10 kg detector can achieve comparable sensitivity to DUNE for $m_\phi \sim$ a few $\times 100$ MeV, while the larger detector can extend the bounds in this mass range to $\lambda \lesssim 10^{-3}$. The proposed detectors also surpass the expected sensitivity of searches for invisible Higgs decays at the HL-LHC [20] and MuCol; see discussion below. This allows us to explore interesting dark matter targets for scalar masses between $m_\phi \sim 1$ MeV and 20 GeV, as discussed in Sec. II. Probing even heavier BSM particles could be possible with a detector operating at a MuCol energy of 10 TeV.

IV. INVISIBLE HIGGS DECAYS

The current constraints on heavy neutrino-philic scalars with mass $m_\phi \gtrsim m_K$ mainly come from measurements of rare weak boson decays [4, 14, 20]. This includes the decay $Z \rightarrow \nu\nu\phi$ which is constrained by the invisible Z branching fraction width measurement at LEP $\text{BR}(Z \rightarrow \text{inv.}) = 20 \pm 0.005\%$ [41]; the decay $W \rightarrow \ell\nu\phi$ which is constrained by the $W \rightarrow \ell\nu$ branching fraction as measured by the LHC [42]; and the decay $h \rightarrow \nu\nu\phi$ (arising from the $\nu\nu\phi h$ term in the Lagrangian) which is constrained by the invisible Higgs branching fraction width measurement at the LHC $\text{BR}(h \rightarrow \text{inv.}) < 0.25$ [43].

A muon collider will likely not improve the measurement of the Z and W decay widths. However, it is expected to improve the measurement of the invisible Higgs decay width. The study performed in Ref. [44] found that a 3 TeV muon collider with luminosity of 2 ab^{-1} could

constrain the BSM contribution to $\text{BR}(h \rightarrow \text{inv.}) < 5 \cdot 10^{-3}$. This assumes that forward muon detectors with a coverage extending to $\eta \sim 5$ are installed on both sides, which would allow to measure the invariant mass of the invisibly decaying Higgs boson.

We can recast this result to obtain a constraint on the neutrino-philic scalar parameter space. The Higgs decay width is given by

$$\Gamma(h \rightarrow \nu_\alpha \nu_\beta \phi) = \frac{4\lambda_{\alpha\beta}^2}{m_h v^2 (1 + \delta_{\alpha\beta})} \int d\Phi_3 |\mathcal{M}|^2 \quad (5)$$

with expressions for the 3-body phase space $d\Phi_3$ and matrix element \mathcal{M} provided in Ref. [20]. Analytically evaluating the integral, we obtain

$$\text{BR}(h \rightarrow \nu_\alpha \nu_\beta \phi) = \frac{1}{\Gamma_h} \frac{\lambda_{\alpha\beta}^2 m_h^3}{3 \cdot 2^7 \pi^3 v^2 (1 + \delta_{\alpha\beta})} \times \left[(1-x)[x(x+10)+1] + 6x(1+x) \log(x) \right], \quad (6)$$

with $x = m_\phi^2/m_h^2$. For $m_\phi \ll m_h$ this simplifies to

$$\text{BR}(h \rightarrow \nu_\alpha \nu_\beta \phi) = \frac{1}{\Gamma_h} \frac{\lambda_{\alpha\beta}^2 m_h^3}{3 \cdot 2^7 \pi^3 v^2 (1 + \delta_{\alpha\beta})}, \quad (7)$$

which agrees with the result obtained in Ref. [4]. Finally, let us note that both the neutrino and anti-neutrino channel contribute to the invisible Higgs decay width, $\text{BR}(h \rightarrow \text{inv.}) = \text{BR}(h \rightarrow \nu\nu\phi) + \text{BR}(h \rightarrow \bar{\nu}\bar{\nu}\phi)$.

Using the projected precision of the muon collider measurement $\text{BR}(h \rightarrow \text{inv.}) < 5 \cdot 10^{-3}$. We can estimate the projected sensitivity reach. For small m_ϕ , the 3 TeV muon collider will be able to probe $\lambda > 0.086$. A full mass dependent sensitivity curve is shown all dash-dotted

line in the right panel of Fig. 1. We can see that it will surpass the sensitivity of LHC measurements. However, measurements using neutrino scattering at a muon collider are expected to be significantly more sensitive.

V. CONCLUSION

Understanding the microscopic nature of the dark sector of the Universe remains the most pressing challenge in particle physics nowadays. Neutrinos have been recognized as a potential portal to this new physics, yet their tiny interaction rates make such endeavors particularly difficult. Powerful neutrino beams, ideally produced in laboratory settings, are needed to test this possibility thoroughly.

To this end, we have proposed to utilize a high-energy neutrino beam expected to be produced in the forward kinematic region of the future Muon Collider to search for a neutrinophilic scalar ϕ , with a mass up to a few tens of GeV. Such scalars could mediate the interaction between dark matter and the Standard Model, providing particularly demanding thermal targets that will miss detection in traditional DM searches. Yet another compelling possibility is that DM is composed of an additional sterile neutrino with a mass of about 10 keV and couplings to the SM driven by the mixing with active neutrinos, which gain substantial self-interaction rates via ϕ . This non-thermal DM target can also be indirectly probed by searching for the mediator ϕ .

We have shown that a compact forward neutrino detector at the MuCol, i.e., the MuCol ν detector, with a mass of about 10 kg, can probe these theory targets even within a year of operation. While the search for the ϕ scalar suffers from substantial neutrino-induced backgrounds, these can be suppressed by several orders of magnitude by observing an apparent lepton-flavor violation in the ϕ production in neutrino scatterings and by imposing further kinematical cuts to isolate signal events that we have discussed in detail.

The expected sensitivity can be further improved by employing a larger target material mass, and we have also

considered discovery prospects for the 10 ton MuCol ν detector. Notably, this also represents the expected sensitivity of, e.g., a 1 ton detector operating for 10 years. This (1 ton) detector mass corresponds to currently operating forward neutrino experiments at the LHC [23, 24, 45–47], while even larger detectors have been proposed for the future Forward Physics Facility at the LHC [25, 48, 49], which would pave the way for the search discussed in this study.

The positive muon production in high-energy muon neutrino scatterings can also be due to the neutrino trident production, however these events will typically be associated with a high-energy negative muon in the final state and will be rejected in our analysis. Dedicated studies of neutrino-trident scattering at high energies, suitable for the FPF era, have been performed in Refs. [50–52] – we expect similarly compelling work focused on MuCol neutrinos in the near future. This will provide a guaranteed physics case for the MuCol ν detector in the near future. Measurements using a MuCol neutrino source (and its very small flux uncertainties) will be highly complementary to those from LHC-produced neutrinos in better understanding the physics underlying neutrino trident scattering.

The forward neutrino beam at the MuCol is by far the largest among all high-energy colliders, offering an unprecedented sensitivity reach in the considered search. This further motivates the work on the proposed forward neutrino detector at the Muon Collider.

ACKNOWLEDGEMENTS

We thank Max Fieg and Andrea Wulzer for sharing the neutrino flux obtained in Ref. [1]. The work of F.K. was supported by the Deutsche Forschungsgemeinschaft under Germany’s Excellence Strategy – EXC 2121 Quantum Universe – 390833306. JA and ST are supported by the National Science Centre, Poland (research grant No. 2021/42/E/ST2/00031). KJK is supported in part by DOE Grant No. DE-SC0010813.

-
- [1] **International Muon Collider** Collaboration, C. Accettura *et al.*, “Interim report for the International Muon Collider Collaboration (IMCC),” [arXiv:2407.12450 \[physics.acc-ph\]](#).
 - [2] **MuCoL** Collaboration, C. Accettura *et al.*, “MuCoL Milestone Report No. 5: Preliminary Parameters,” [arXiv:2411.02966 \[physics.acc-ph\]](#).
 - [3] J. M. Berryman *et al.*, “Neutrino self-interactions: A white paper,” *Phys. Dark Univ.* **42** (2023) 101267, [arXiv:2203.01955 \[hep-ph\]](#).
 - [4] J. M. Berryman, A. De Gouvêa, K. J. Kelly, and Y. Zhang, “Lepton-Number-Charged Scalars and Neutrino Beamstrahlung,” *Phys. Rev. D* **97** (2018) no. 7, 075030, [arXiv:1802.00009 \[hep-ph\]](#).
 - [5] K. J. Kelly and Y. Zhang, “Mononeutrino at DUNE: New Signals from Neutrinophilic Thermal Dark Matter,” *Phys. Rev. D* **99** (2019) no. 5, 055034, [arXiv:1901.01259 \[hep-ph\]](#).
 - [6] K. J. Kelly, F. Kling, D. Tuckler, and Y. Zhang, “Probing neutrino-portal dark matter at the Forward Physics Facility,” *Phys. Rev. D* **105** (2022) no. 7, 075026, [arXiv:2111.05868 \[hep-ph\]](#).
 - [7] S. Dodelson and L. M. Widrow, “Sterile-neutrinos as dark matter,” *Phys. Rev. Lett.* **72** (1994) 17–20, [arXiv:hep-ph/9303287](#).

- [8] A. De Gouvêa, M. Sen, W. Tangarife, and Y. Zhang, “Dodelson-Widrow Mechanism in the Presence of Self-Interacting Neutrinos,” *Phys. Rev. Lett.* **124** (2020) no. 8, 081802, [arXiv:1910.04901 \[hep-ph\]](#).
- [9] K. J. Kelly, M. Sen, and Y. Zhang, “Intimate Relationship between Sterile Neutrino Dark Matter and ΔN_{eff} ,” *Phys. Rev. Lett.* **127** (2021) no. 4, 041101, [arXiv:2011.02487 \[hep-ph\]](#).
- [10] K. J. Kelly, M. Sen, W. Tangarife, and Y. Zhang, “Origin of sterile neutrino dark matter via secret neutrino interactions with vector bosons,” *Phys. Rev. D* **101** (2020) no. 11, 115031, [arXiv:2005.03681 \[hep-ph\]](#).
- [11] R. An, V. Gluscevic, E. O. Nadler, and Y. Zhang, “Can Neutrino Self-interactions Save Sterile Neutrino Dark Matter?,” *Astrophys. J. Lett.* **954** (2023) no. 1, L18, [arXiv:2301.08299 \[astro-ph.CO\]](#).
- [12] N. Blinov, K. J. Kelly, G. Z. Krnjaic, and S. D. McDermott, “Constraining the Self-Interacting Neutrino Interpretation of the Hubble Tension,” *Phys. Rev. Lett.* **123** (2019) no. 19, 191102, [arXiv:1905.02727 \[astro-ph.CO\]](#).
- [13] G. Barenboim, “Inflation might be caused by the right: Handed neutrino,” *JHEP* **03** (2009) 102, [arXiv:0811.2998 \[hep-ph\]](#).
- [14] V. Brdar, M. Lindner, S. Vogl, and X.-J. Xu, “Revisiting neutrino self-interaction constraints from Z and τ decays,” *Phys. Rev. D* **101** (2020) no. 11, 115001, [arXiv:2003.05339 \[hep-ph\]](#).
- [15] P. S. B. Dev, D. Kim, D. Sathyan, K. Sinha, and Y. Zhang, “New Laboratory Constraints on Neutrinophilic Mediators,” [arXiv:2407.12738 \[hep-ph\]](#).
- [16] **PIENU** Collaboration, A. Aguilar-Arevalo *et al.*, “Search for three body pion decays $\pi^+ \rightarrow l^+ \nu X$,” *Phys. Rev. D* **103** (2021) no. 5, 052006, [arXiv:2101.07381 \[hep-ex\]](#).
- [17] **NA62** Collaboration, E. Cortina Gil *et al.*, “Search for K^+ decays to a muon and invisible particles,” *Phys. Lett. B* **816** (2021) 136259, [arXiv:2101.12304 \[hep-ex\]](#).
- [18] I. Esteban, S. Pandey, V. Brdar, and J. F. Beacom, “Probing secret interactions of astrophysical neutrinos in the high-statistics era,” *Phys. Rev. D* **104** (2021) no. 12, 123014, [arXiv:2107.13568 \[hep-ph\]](#).
- [19] W. Bai, J. Liao, and H. Liu, “Constraining neutrinophilic mediators at **FASER** ν , **FLArE** and **FASER** $\nu 2$,” [arXiv:2409.01826 \[hep-ph\]](#).
- [20] A. de Gouvêa, P. S. B. Dev, B. Dutta, T. Ghosh, T. Han, and Y. Zhang, “Leptonic Scalars at the LHC,” *JHEP* **07** (2020) 142, [arXiv:1910.01132 \[hep-ph\]](#).
- [21] Y. Hamada, R. Kitano, R. Matsudo, H. Takaura, and M. Yoshida, “ μ TRISTAN,” *PTEP* **2022** (2022) no. 5, 053B02, [arXiv:2201.06664 \[hep-ph\]](#).
- [22] C. H. de Lima, D. McKeen, J. N. Ng, M. Shamma, and D. Tucker, “Probing Lepton Number Violation at Same-Sign Lepton Colliders,” [arXiv:2411.15303 \[hep-ph\]](#).
- [23] **FASER** Collaboration, H. Abreu *et al.*, “Detecting and Studying High-Energy Collider Neutrinos with **FASER** at the LHC,” *Eur. Phys. J. C* **80** (2020) no. 1, 61, [arXiv:1908.02310 \[hep-ex\]](#).
- [24] **SND@LHC** Collaboration, G. Acampora *et al.*, “**SND@LHC**: the scattering and neutrino detector at the LHC,” *JINST* **19** (2024) no. 05, P05067, [arXiv:2210.02784 \[hep-ex\]](#).
- [25] J. L. Feng *et al.*, “The Forward Physics Facility at the High-Luminosity LHC,” *J. Phys. G* **50** (2023) no. 3, 030501, [arXiv:2203.05090 \[hep-ex\]](#).
- [26] R. Mammen Abraham, J. Adhikary, J. L. Feng, M. Fieg, F. Kling, J. Li, J. Pei, T. R. Rabemananjara, J. Rojo, and S. Trojanowski, “**FPF@FCC**: Neutrino, QCD, and BSM Physics Opportunities with Far-Forward Experiments at a 100 TeV Proton Collider,” [arXiv:2409.02163 \[hep-ph\]](#).
- [27] B. Batell, H. Davoudiasl, R. Marcarelli, E. T. Neil, and S. Trojanowski, “Lepton-flavor-violating ALP signals with TeV-scale muon beams,” *Phys. Rev. D* **110** (2024) no. 7, 075039, [arXiv:2407.15942 \[hep-ph\]](#).
- [28] B. J. King, “Neutrino physics at a muon collider,” *AIP Conf. Proc.* **435** (1998) no. 1, 334–348, [arXiv:hep-ex/9907033](#).
- [29] **FASER** Collaboration, H. Abreu *et al.*, “First Direct Observation of Collider Neutrinos with **FASER** at the LHC,” *Phys. Rev. Lett.* **131** (2023) no. 3, 031801, [arXiv:2303.14185 \[hep-ex\]](#).
- [30] **SND@LHC** Collaboration, R. Albanese *et al.*, “Observation of Collider Muon Neutrinos with the **SND@LHC** Experiment,” *Phys. Rev. Lett.* **131** (2023) no. 3, 031802, [arXiv:2305.09383 \[hep-ex\]](#).
- [31] **FASER** Collaboration, R. Mammen Abraham *et al.*, “First Measurement of νe and $\nu \mu$ Interaction Cross Sections at the LHC with **FASER**’s Emulsion Detector,” *Phys. Rev. Lett.* **133** (2024) no. 2, 021802, [arXiv:2403.12520 \[hep-ex\]](#).
- [32] J. Alwall, R. Frederix, S. Frixione, V. Hirschi, F. Maltoni, O. Mattelaer, H. S. Shao, T. Stelzer, P. Torrielli, and M. Zaro, “The automated computation of tree-level and next-to-leading order differential cross sections, and their matching to parton shower simulations,” *JHEP* **07** (2014) 079, [arXiv:1405.0301 \[hep-ph\]](#).
- [33] K. Kovarik *et al.*, “**nCTEQ15** - Global analysis of nuclear parton distributions with uncertainties in the CTEQ framework,” *Phys. Rev. D* **93** (2016) no. 8, 085037, [arXiv:1509.00792 \[hep-ph\]](#).
- [34] T. Sjöstrand, S. Ask, J. R. Christiansen, R. Corke, N. Desai, P. Ilten, S. Mrenna, S. Prestel, C. O. Rasmussen, and P. Z. Skands, “An introduction to **PYTHIA 8.2**,” *Comput. Phys. Commun.* **191** (2015) 159–177, [arXiv:1410.3012 \[hep-ph\]](#).
- [35] **Particle Data Group** Collaboration, S. Navas *et al.*, “Review of particle physics,” *Phys. Rev. D* **110** (2024) no. 3, 030001.
- [36] A. Candido, A. Garcia, G. Magni, T. Rabemananjara, J. Rojo, and R. Stegeman, “Neutrino Structure Functions from GeV to EeV Energies,” *JHEP* **05** (2023) 149, [arXiv:2302.08527 \[hep-ph\]](#).
- [37] J. M. Cruz-Martinez, M. Fieg, T. Giani, P. Krack, T. Mäkelä, T. R. Rabemananjara, and J. Rojo, “The LHC as a Neutrino-Ion Collider,” *Eur. Phys. J. C* **84** (2024) no. 4, 369, [arXiv:2309.09581 \[hep-ph\]](#).
- [38] A. Accardi *et al.*, “Electron Ion Collider: The Next QCD Frontier: Understanding the glue that binds us all,” *Eur. Phys. J. A* **52** (2016) no. 9, 268, [arXiv:1212.1701 \[nucl-ex\]](#).
- [39] **FASER** Collaboration, A. Ariga *et al.*, “Technical Proposal for **FASER**: ForwArd Search Experiment at

- the LHC,” [arXiv:1812.09139 \[physics.ins-det\]](#).
- [40] F. Pedregosa, G. Varoquaux, A. Gramfort, V. Michel, B. Thirion, O. Grisel, M. Blondel, P. Prettenhofer, R. Weiss, V. Dubourg, J. Vanderplas, A. Passos, D. Cournapeau, M. Brucher, M. Perrot, and E. Duchesnay, “Scikit-learn: Machine learning in Python,” *Journal of Machine Learning Research* **12** (2011) 2825–2830.
- [41] **LEP, ALEPH, DELPHI, L3, OPAL, LEP Electroweak Working Group, SLD Electroweak Group, SLD Heavy Flavor Group** Collaboration, t. S. Electroweak, “A Combination of preliminary electroweak measurements and constraints on the standard model,” [arXiv:hep-ex/0312023](#).
- [42] **ATLAS** Collaboration, M. Aaboud *et al.*, “Measurement of the W -boson mass in pp collisions at $\sqrt{s} = 7$ TeV with the ATLAS detector,” *Eur. Phys. J. C* **78** (2018) no. 2, 110, [arXiv:1701.07240 \[hep-ex\]](#). [Erratum: *Eur.Phys.J.C* 78, 898 (2018)].
- [43] **CMS** Collaboration, V. Khachatryan *et al.*, “Searches for invisible decays of the Higgs boson in pp collisions at $\sqrt{s} = 7, 8,$ and 13 TeV,” *JHEP* **02** (2017) 135, [arXiv:1610.09218 \[hep-ex\]](#).
- [44] M. Ruhdorfer, E. Salvioni, and A. Wulzer, “Invisible Higgs boson decay from forward muons at a muon collider,” *Phys. Rev. D* **107** (2023) no. 9, 095038, [arXiv:2303.14202 \[hep-ph\]](#).
- [45] **FASER** Collaboration, H. Abreu *et al.*, “Technical Proposal: FASERnu,” [arXiv:2001.03073 \[physics.ins-det\]](#).
- [46] **FASER** Collaboration, H. Abreu *et al.*, “The FASER detector,” *JINST* **19** (2024) no. 05, P05066, [arXiv:2207.11427 \[physics.ins-det\]](#).
- [47] C. Ahdida *et al.*, “SND@LHC - Scattering and Neutrino Detector at the LHC,” <https://cds.cern.ch/record/2750060>.
- [48] L. A. Anchordoqui *et al.*, “The Forward Physics Facility: Sites, experiments, and physics potential,” *Phys. Rept.* **968** (2022) 1–50, [arXiv:2109.10905 \[hep-ph\]](#).
- [49] J. Adhikary *et al.*, “Science and Project Planning for the Forward Physics Facility in Preparation for the 2024-2026 European Particle Physics Strategy Update,” [arXiv:2411.04175 \[hep-ex\]](#).
- [50] R. Francener, V. P. Goncalves, and D. R. Gratieri, “Neutrino trident scattering at the LHC energy regime,” *Eur. Phys. J. C* **84** (2024) no. 9, 923, [arXiv:2406.13593 \[hep-ph\]](#).
- [51] W. Altmannshofer, T. Mäkelä, S. Sarkar, S. Trojanowski, K. Xie, and B. Zhou, “Discovering neutrino tridents at the Large Hadron Collider,” *Phys. Rev. D* **110** (2024) no. 7, 072018, [arXiv:2406.16803 \[hep-ph\]](#).
- [52] I. Bigaran, P. S. B. Dev, D. Lopez Gutierrez, and P. A. N. Machado, “Tau Tridents at Accelerator Neutrino Facilities,” [arXiv:2406.20067 \[hep-ph\]](#).